



GEOMETRY OPTIMIZATION AND VIBRATIONAL FREQUENCIES OF TETRACENE MOLECULE IN GAS PHASE AND IN METHANOL BASED ON DENSITY FUNCTIONAL THEORY AND RESTRICTED HARTREE-FOCK

¹Gidado, A.S., ²Abubakar Maigari and ¹Galadanci, G.S.M.

¹Department of Physics, Bayero University, Kano PMB 3011

²College of Education, Azare PMB 044, Bauchi State

*Correspondence author: asgidado.phy@buk.edu.ng

ABSTRACT

Tetracene is an organic semiconductor with chemical formula $C_{18}H_{12}$ used in organic field effect-transistor (OFET) and organic light emitting diode (OLED). In this work, the molecular geometry (optimized bond lengths and bond angles), vibrational frequencies and intensities, HOMO-LUMO Energy gap and Atomic charge distribution of the Tetracene molecule in gas phase and in solution were calculated and reported. Restricted Hartree-Fock (RHF) and Density Functional Theory (DFT) with different basis sets were employed for the task. Windows version of Gaussian 03 software was used to perform all the calculations. The results obtained show that the bond length obtained using RHF has the lowest average value of 1.072Å and that obtained using DFT has the lowest average value of 1.085Å in gas phase. In Methanol, it is observed that at RHF level, the lowest average value was 1.075Å and at DFT level was 1.087Å. This shows that the values are a bit higher in methanol than in gas phase which implies that the bonds will be slightly stronger in gas phase than in methanol. The strongest bonds in tetracene molecule are those of C20-H28, C23-H29 and C24-H30 in both gas and methanol. The weakest bonds are those of C6-C12 and C6-C14. The bond angles were found to be so closed to 120° at both levels of theory for all basis sets used suggesting that the molecule is planar benzene in which the C atoms are sp^2 hybridized. The calculated HOMO-LUMO energy gap shows that the molecule will be slightly more stable in chemical reaction in gas phase than in methanol. DFT values of the energy gap appeared to be closer to the reported experimental value of 2.6eV than those obtained by RHF. The atomic charges distribution was found to be very sensitive to the basis sets which presumably occur due to polarization. From the results obtained for vibrational frequencies, it shows that tetracene molecule would be more stable in gas phase than in methanol as a result of no imaginary frequency found in gas phase. This confirms the stability of the molecule as stated in the results of HOMO-LUMO energy gap. The calculated vibrational frequencies show that the most intense frequency was obtained to be 924.9862 cm^{-1} at 146.7973KM/mole by RHF/3-21G in gas phase while at B3LYP/3-21G, it has the most intense frequency of about 474.1260 cm^{-1} at 390.1077.2845MK/mole in methanol.

Keywords: Optimisation, Methanol, Gas, Frequency, Tetracene

INTRODUCTION

Organic semiconductor materials (OSM) such as oligoacenes, a subclass of polyaromatic hydrocarbon are made of fused of benzene rings joined in a linear arrangement (Cappellin *et. al.*, 2009) hold a great promising benefit as active elements in a variety of electronic and optoelectronic devices (Yumusak *et. al.*, 2012) . In general, one of the most important advantages of organic materials instead of inorganic materials is its low cost, low temperature and solution-based processing. Among the organic compounds, polyacenes demonstrate a promising results as the ideal case due to their simple structure and they find several applications in organic thin films field effect transistors, organic light-emitting diode (OLEDs), solar cell, e.t.c . Also, acene ring based on tetracene molecule was reported to exhibit superconducting properties at low temperature. Moreover, Organic semiconductors have been intensely researched for two decades because they are key components in organic field-effect transistors (OFETs) which are necessary for next-generation electronics, such as flexible sensors. The term organic semiconductors implies that the materials are mostly

made up by carbon and hydrogen atoms, with a few heteroatom such as sulfur, oxygen and nitrogen included and they show properties typically associated with a semiconductor materials (Anna and Heinz, 2015).

Conduction mechanisms for organic semiconductor are mainly through tunneling; hopping between localized states, mobility gaps, and phonon assisted hopping. Like inorganic semiconductors, organic semiconductors can be doped in order to change its conductivity. Although inorganic semiconductors such as silicon, germanium and gallium arsenide have been the backbone of semiconductor industry, for the past decade, demands for pervasive computing have led to a dramatic improvement in the performance of organic semiconductor. Organic semiconductors have been used as active elements in optoelectronic devices such as organic light emitting diodes (OLED), organic solar cells, and organic field effect transistors (OFET). There are many advantages of using organic semiconductors, such as easy fabrication, mechanical flexibility, and low cost.

Organic semiconductors offer the ability to fabricate electronic device at lower temperature and over large areas on various flexible substrate such as plastic and paper. They can be processed using existing techniques used in semi conducting industry as well as in printing industries such as roll-to-roll manufacturing.

However, the mobility of organic semiconductor cannot match the performance of field-effect transistors based on single-crystalline inorganic semiconductor such as silicon or germanium. These inorganic semiconductors have charge carrier mobilities nearly three order of magnitude higher than typical organic semiconductor (Mason *et. al*, 2002). As a result of this limitation, organic semiconductors are not suitable for use in electronic applications that require very high switching speeds. However, the performance of some organic semiconductors, coupled with their ease of processing makes it competitive in electronic applications that do not require high switching speed such as amorphous silicon. Organic semiconductors can be divided into two types, short chain (oligomers) and long chain (polymers) (Shaw and Seidler, 2001). Typical examples for semiconducting oligomers are pentacene, anthracene, tetracene, and rubrene. Some semiconducting polymers are Poly (3- hexylthiophene) and poly (p-phenylene vinylene).

Short chain organic semiconductors are usually formed by a series of benzene rings in which the π -bonds become delocalized to form a π -system. Long chain organic semiconductors are usually polymers

that are delocalized along the chain to form a one-dimensional system resulting in a 1D-band structure that has considerable band width. The transport properties of such polymers are usually determined by defects in the 1D-chains or by hopping from chain to chain. Polymer organic semiconductors are usually deposited in wet processes, like spin coating or doctor blading.

Tetracene has been identified as an organic semiconductor with chemical formula $C_{18}H_{12}$. It is a polycyclic aromatic hydrocarbon. Tetracene is a molecular organic semiconductor, used in organic field-effect transistors (DEFTs) and organic light-emitted diode (OLEDs). In May 2007, researchers from two Japanese universities, Tohoku University in Sendai and Osaka University, reported an ambipolar light-emitting transistor made of a single tetracene crystal (Takashi *et al.*, 2007). Ambipolar means that the electric charge is transported by both positively charged holes and negatively charged electrons. Tetracene can also be used as a gain medium in dye lasers as sensitizer in chemo luminescence. Jan Hendrik Schön during his time at Bell Labs (1997–2002) claimed to have developed an electrically pumped laser based on tetracene. In February 2014, National Aeronautic and space Agency (NASA) announced a greatly upgraded database for tracking polycyclic aromatic hydrocarbons (PAHs), including Tetracene, in the universe (Hoover, 2014). The frontier orbital (LUMO and HOMO) energies of tetracene molecule have been investigated and reported by (Peter *et al.*, 2009 and Musa *et al.*, 2015).

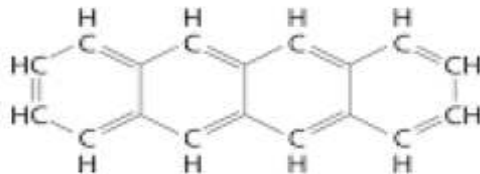


Figure 1. Structure of Tetracene molecule

In this work, geometry optimization and vibrational analysis of tetracene neutral molecule in order to find out the effects in both gas phase and in methanol are intended to be carried out. The effects of different levels of theory and basis sets will also be investigated.

THEORETICAL BACKGROUND

Density Functional Theory (DFT)

Density Functional Theory (DFT) is a computational method that derives properties of the molecules based on the determination of their electron density. DFT methods have become the most widely-spread *ab-initio* methods in Computational Materials Science (CMS) and Solid state Physics, due to their high computational efficiency and very good accuracy for the structure of molecules, crystals, surfaces and their interactions. In DFT methods, the energy of the molecule is a functional of the electron density (Gidado *et al.*, 2015).

Vibrational Frequency

The vibrational frequencies are calculated with the following equations (Gidado *et. al.*, 2015)

$$V_{ij} = \frac{1}{\sqrt{m_i m_j}} \left(\frac{\partial^2 V}{\partial q_i \partial q_j} \right) \quad (1)$$

where V_{ij} is the Hessian matrix, m_i refers to the mass of atom i , and ∂_{q_i} refers to a displacement of atom i in the x -, y -, or z -direction,

$$VU = \lambda U \quad (2)$$

where U is a matrix of eigenvectors and λ is a vector of eigen values, and

$$\lambda_k = (2\pi\nu_k)^2 \quad (3)$$

Where λ_k is the k^{th} eigen value and ν_k is the k^{th} vibrational frequency.

The infrared intensities can be computed with the equation (Gidado *et al.*, 2015)

$$\frac{\partial E_{SCF}}{\partial f \partial a} = 2 \sum_i^{d.o} h_{ij}^{fa} + 4 \sum_i^{d.o} \sum_j^{all} U_{ji}^a h_{ij}^f \quad (4)$$

$$h_{ij}^{fa} = \sum_{\mu\nu}^{AO} C_{\mu}^{i0} C_{\nu}^{j0} \left(\frac{\partial^2 h_{\mu\nu}}{\partial f \partial a} \right) \quad (5)$$

where

E_{SCF} is the self-consistent field energy, f is the electric field, a is a nuclear coordinate, $h_{\mu\nu}$ is the one-electron atomic orbital integral, U^p is related to the derivative of the molecular orbital coefficients with respect to a by

$$\frac{\partial C_{\mu}^i}{\partial a} = \sum_m^{all} U_{mi}^a C_{\mu}^{m0} \quad (6)$$

The term "all" in the above summations refers to all occupied and virtual molecular orbitals and .d.o... Refers to doubly occupied orbitals such as those found in the ground state of a closed-shell system.

Terms such as C_{μ}^{i0} refers to the coefficients of the atomic orbital m in the i th unperturbed molecular orbital.

HOMO-LUMO Energy

The Highest occupied molecular orbital energy (HOMO) and lowest unoccupied molecular orbital energy (LUMO) are very popular quantum chemical parameters. These orbital's, also called the frontier orbital's, determine the way the molecule interacts with other species. The HOMO is the orbital that could act as an electron donor, since it is the outermost (highest energy) orbital containing electrons. The LUMO is the orbital that could act as the electron acceptor, since it is the innermost (lowest energy) orbital that has room to accept electrons. According to the frontier molecular orbital theory, the formation of a transition state is due to an interaction between the frontier orbital's (HOMO and LUMO) of reactants. The energy of the HOMO is directly related to the ionization potential and the energy of the LUMO is directly related to the electron affinity. The HOMO-LUMO gap, that is the difference in energy between the HOMO and LUMO, is an important stability index. A large HOMO-LUMO gap implies high stability for the molecule in chemical reactions. The concept of "activation hardness" has been also defined on the basis of the HOMO-LUMO energy gap. The qualitative definition of hardness is closely related to the polarizability, since a decrease of the energy gap usually leads to easier polarization of the molecule. The HOMO-LUMO gap is defined as (Gidado *et. al.*, 2015)

$$\Delta E = E_{LUMO} - E_{HOMO}$$

Where

ΔE = Is the HOMO-LUMO gap energy

E_{HOMO} = Is the HOMO energy

E_{LUMO} = Is the LUMO energy

MATERIALS AND METHODS

All computations were carried out using Windows Version of Gaussian 03 software (Frisch *et al.*, 2004). The molecular structures and geometries of tetracene have been completely optimized using ab-initio quantum mechanical calculations at the Restricted Hartree-Fock (RHF) and Density Functional Theory (DFT) level of theory without using any symmetry constraints using various basis sets. Gaussian 03 software is a computational Physics and Chemistry

program that is used for electronic and geometric structure optimization (geometry optimization, transition states, single point calculation and reaction path modeling), molecular properties, vibrational analysis, electrostatic potential, electron density, and multi-pole moment e.t.c. using both DFT and RHF methods. Geometry optimizations were performed using RHF and DFT levels of theory with different basis sets such as 6-31G, 6-31G (d), 6-31+G and 6-31G(d,p) . A basis set is a set of wave functions that described the shape of atomic orbital's (AOs). The Density Functional Theory is a cost effective method for inclusion of electron correlations. Geometry optimization is a name for the procedure that attempts to find the configuration of minimum energy of the molecule. The procedure calculated the wave function and the energy at the starting geometry and then proceeded to search a new geometry of a lower energy. This was repeated until the lowest energy geometry was found. In a nut shell geometry optimization was done by locating both the minima and transition states on the potential surface of the molecular orbitals. The optimized molecule obtained from geometry optimization was used as the starting geometry for vibrational calculations. The vibrational analysis was performed by computing the Hessian matrix and the force constants for all the normal modes of the molecule. The frequencies were scaled with a factor of 0.89 in order to remove the effect of the harmonic oscillator. Frequency job began by computing the energy of the input structure. It then went on to compute the frequencies for the structures. Gaussian predicted the frequencies and intensities of each spectral line. The HOMO-LUMO Energy was calculated and from which the energy gap was calculated as the difference in energy between the HOMO and LUMO. IRPal 2.0 was used to interpret the spectra. (7)

RESULTS AND DISCUSSION

Optimized bond lengths (Å) of Tetracene Molecule in Gas Phase and methanol

The optimized bond lengths of tetracene molecule at two different levels of theory (RHF and B3LYP) in gas phase and Methanol are listed in Tables 1 and 2. The bond length is the measurable distance between two atoms covalently bonded together. It is worth noting that the shorter the bond length the higher is the value of the bond energy (Suzuki *et.al*, 2006). The results obtained show that the bond lengths using RHF method has the lowest average value of 1.072Å and at DFT level has the lowest average value of 1.085Å in the gas phase. In Methanol, it is observed that at RHF level, the lowest average value was 1.075Å and at DFT level, it was 1.087Å.

This indicates that the values are a bit higher in methanol than in gas the phase which implies that the bonds will be slightly stronger in the gas phase than in solution form.

Table1 also shows that the basis set 3-21G gives the lowest values of the bond lengths and 6-31G+ gives the highest values of the bond lengths at RHF level of theory. It is observed that the bonds R(20,28):C20-H28 and R(23,29):C23-H29 follow by R(13,21):C23-H21, R(14,22):C14-H22, and R(17,25):C17-H25 between carbon and hydrogen atoms at the indicated positions have the lowest values of bond lengths ranging from 1.0717Å to 1.0728Å. Similarly for B3LYP level of theory, the basis set 3-21G gives the lowest values of the bond lengths and 6-31G+ gives the highest values. It is predicted that the bonds R(13,21);C13-H21 and R(14,22):C14-H22 follow by R(7,15) and R(19,27) between carbon and hydrogen atoms at the indicated positions possess the lowest values of the bond lengths ranging between 1.0853Å to 1.085Å. These are the strongest bonds and have the largest values of bond energy in the Tetracene molecule which cannot be easily broken. A large amount of energy is needed to break them. On the other hand, at both levels of theory, the bonds R(6,14):C6-C14, R(12,18):C12-C18, R(20,24):C20-C24, and R(1,2):C1-C2, R(5,11):C5-C11, R(6,12):C6-C12 between Carbon-Carbon atoms at the specified

positions have the highest values of bond lengths ranging from 1.4425Å to 1.4557Å. These are the weakest bonds and less amount of energy are required to break them.

Similarly, Table 2 shows that at both levels of theory (RHF and DFT), the basis sets 3-21G and 3-21G+ give the least values of the bond lengths and 6-31G gives the highest values. It is predicted that the bonds R (4, 10):C4-H10, R (7, 15):C7-H15, R (13, 21):C13-H21 and R (17, 25):C17-H25 between Carbon and Hydrogen atoms at the specified positions have the lowest values of bond lengths ranging from 1.0753Å to 1.0762Å at RHF/3-21G. Similarly the bonds R (24, 30):C24-H30, R (23, 29):C23-H29 and R (20, 28):C20-H28 between Carbon and Hydrogen atoms at the indicated positions possess the least values of bond lengths ranging within 1.0863Å at B3LYP/3-21G+. These are the strongest and hence have the largest values of bond energy in Tetracene molecule which cannot be easily broken. On the other hand, the bonds R (5, 13):C5-C13, R (11, 17):C11-C17, R (1, 2):C1-C2 and R (5, 11) between Carbon-Carbon atoms at the specified positions have the highest values ranging from 1.4441Å at RHF to 1.4569Å at B3LYP. These are the weakest and hence have the lowest values of bond energy. Therefore less amount of energy will be required to break them.

Table 1: Optimized Bond Lengths (Å) of Tetracene Molecule Gas Phase

Bond lengths	RHF				B3LYP			
	3-21G	3-21G+	6-31G	6-31G+	3-21G	3-21G+	6-31G	6-31G+
R(1,2)	1.4287	1.4287	1.4309	1.4313	1.4557	1.456	1.4563	1.4567
R(1,3)	1.4055	1.4055	1.4078	1.409	1.4109	1.4125	1.413	1.4143
R(1,4)	1.4056	1.4056	1.4078	1.409	1.4109	1.4125	1.413	1.4143
R(2,7)	1.4055	1.4055	1.4078	1.409	1.4109	1.4125	1.413	1.4143
R(2,8)	1.4056	1.4056	1.4078	1.409	1.4109	1.4125	1.413	1.4143
R(3,6)	1.3722	1.3722	1.3774	1.3787	1.3924	1.3943	1.3961	1.3974
R(3,9)	1.0736	1.0736	1.0747	1.0751	1.0858	1.0876	1.0872	1.0877
R(4,5)	1.3721	1.3721	1.3773	1.3787	1.3924	1.3943	1.3961	1.3973
R(4,10)	1.0736	1.0736	1.0747	1.0751	1.0858	1.0876	1.0872	1.0877
R(5,11)	1.4373	1.4373	1.4387	1.4393	1.4547	1.4555	1.4556	1.4563
R(5,13)	1.4425	1.4425	1.4417	1.4427	1.4363	1.4378	1.4366	1.438
R(6,12)	1.4372	1.4372	1.4387	1.4393	1.4547	1.4555	1.4556	1.4563
R(6,14)	1.4425	1.4425	1.4417	1.4426	1.4363	1.4378	1.4366	1.438
R(7,12)	1.3722	1.3722	1.3774	1.3787	1.3924	1.3943	1.3961	1.3974
R(7,15)	1.0736	1.0736	1.0747	1.0751	1.0858	1.0876	1.0872	1.0877
R(8,11)	1.3721	1.3721	1.3773	1.3787	1.3924	1.3943	1.3961	1.3973
R(8,16)	1.0736	1.0736	1.0747	1.0751	1.0858	1.0876	1.0872	1.0877
R(11,17)	1.4425	1.4425	1.4417	1.4427	1.4363	1.4378	1.4366	1.438
R(12,18)	1.4425	1.4425	1.4417	1.4426	1.4363	1.4378	1.4366	1.438
R(13,19)	1.3414	1.3414	1.3479	1.3499	1.3662	1.3692	1.3712	1.3731
R(13,21)	1.0728	1.0728	1.0739	1.0742	1.085	1.0865	1.0864	1.0869
R(14,20)	1.3414	1.3414	1.3479	1.35	1.3662	1.3692	1.3712	1.3731
R(14,22)	1.0728	1.0728	1.0739	1.0742	1.085	1.0865	1.0864	1.0869
R(17,23)	1.3414	1.3414	1.3479	1.3499	1.3662	1.3692	1.3712	1.3731
R(17,25)	1.0728	1.0728	1.0739	1.0742	1.085	1.0865	1.0864	1.0869
R(18,24)	1.3414	1.3414	1.3479	1.35	1.3662	1.3692	1.3712	1.3731

Table 1 continue

Bond lengths	RHF				B3LYP			
	3-21G	3-21G+	6-31G	6-31G+	3-21G	3-21G+	6-31G	6-31G+
R(18,26)	1.0728	1.0728	1.0739	1.0742	1.085	1.0865	1.0864	1.0869
R(19,23)	1.439	1.439	1.4376	1.4386	1.4327	1.4348	1.433	1.4345
R(19,27)	1.0717	1.0717	1.0729	1.0732	1.0838	1.0853	1.0853	1.0857
R(20,24)	1.439	1.439	1.4376	1.4386	1.4327	1.4348	1.433	1.4345
R(20,28)	1.0717	1.0717	1.0729	1.0732	1.0838	1.0853	1.0853	1.0857
R(23,29)	1.0717	1.0717	1.0729	1.0732	1.0838	1.0853	1.0853	1.0857
R(24,30)	1.0717	1.0717	1.0729	1.0732	1.0838	1.0853	1.0853	1.0857

Table 2: Optimized Bond Lengths (Å) of Tetracene Molecule in Methanol.

Bond lengths	RHF				B3LYP			
	3-21G	3-21G+	6-31G	6-31G+	3-21G	3-21G+	6-31G	6-31G+
R(1,2)	1.4302	1.4302	1.4322	1.4291	1.4571	1.4571	1.0863	1.4537
R(1,3)	1.407	1.407	1.4092	1.4095	1.4124	1.4124	1.4143	1.4115
R(1,4)	1.407	1.407	1.4092	1.4095	1.4124	1.4124	1.4143	1.4115
R(2,7)	1.407	1.407	1.4092	1.4095	1.4124	1.4124	1.4143	1.4115
R(2,8)	1.407	1.407	1.4092	1.375	1.4124	1.4124	1.4143	1.4115
R(3,6)	1.3737	1.3737	1.3788	1.0786	1.3939	1.3939	1.3974	1.3939
R(3,9)	1.0762	1.0762	1.0769	1.3749	1.0885	1.0885	1.0894	1.0904
R(4,5)	1.3737	1.3737	1.3788	1.0786	1.3939	1.3939	1.3974	1.3939
R(4,10)	1.0762	1.0762	1.0769	1.4395	1.0885	1.0885	1.0894	1.0904
R(5,11)	1.4388	1.4388	1.4401	1.4457	1.4562	1.4562	1.4569	1.4532
R(5,13)	1.4441	1.4441	1.4431	1.4395	1.4379	1.4379	1.4381	1.4353
R(6,12)	1.4388	1.4388	1.44	1.4457	1.4562	1.4562	1.4569	1.4532
R(6,14)	1.444	1.444	1.4431	1.375	1.4379	1.4379	1.4381	1.4353
R(7,12)	1.3737	1.3737	1.3788	1.0786	1.3939	1.3939	1.3974	1.3939
R(7,15)	1.0762	1.0762	1.0769	1.3749	1.0885	1.0885	1.0894	1.0904
R(8,11)	1.3737	1.3737	1.3788	1.0786	1.3939	1.3939	1.3974	1.3939
R(8,16)	1.0762	1.0762	1.0769	1.4457	1.0885	1.0885	1.0894	1.0904
R(11,17)	1.4441	1.4441	1.4431	1.4457	1.4379	1.4379	1.4381	1.4353
R(12,18)	1.444	1.444	1.4431	1.3437	1.4379	1.4379	1.4381	1.4353
R(13,19)	1.3429	1.3429	1.3494	1.078	1.3677	1.3677	1.3726	1.3683
R(13,21)	1.0753	1.0753	1.0762	1.3438	1.0876	1.0876	1.0887	1.0898
R(14,20)	1.3429	1.3429	1.3494	1.078	1.3677	1.3677	1.3726	1.3683
R(14,22)	1.0753	1.0753	1.0762	1.3437	1.0876	1.0876	1.0887	1.0898
R(17,23)	1.3429	1.3429	1.3494	1.3437	1.3677	1.3677	1.3726	1.3683
R(17,25)	1.0753	1.0753	1.0762	1.078	1.0876	1.0876	1.0887	1.0898
R(18,24)	1.3429	1.3429	1.3494	1.3438	1.3677	1.3677	1.3726	1.3683
R(18,26)	1.0753	1.0753	1.0762	1.078	1.0876	1.0876	1.0887	1.0898
R(19,23)	1.4408	1.4408	1.4393	1.4435	1.4345	1.4345	1.4347	1.4323
R(19,27)	1.0742	1.0742	1.0751	1.0773	1.0863	1.0863	1.0876	1.0888
R(20,24)	1.4407	1.4407	1.4393	1.4434	1.4345	1.4345	1.4346	1.4323
R(20,28)	1.0742	1.0742	1.0751	1.0773	1.0863	1.0863	1.0876	1.0888
R(23,29)	1.0742	1.0742	1.0751	1.0773	1.0863	1.0863	1.0876	1.0888
R(24,30)	1.0742	1.0742	1.0751	1.0773	1.0863	1.0863	1.0876	1.0888

Optimized bond angle (Å) of Tetracene molecule in gas phase and in methanol

The optimized bond angles of tetracene molecule at both levels of theory (RHF and B3LYP) in gas phase and methanol are listed in Table 3 and 4. The bond angle is the average angle between the orbitals of the

central atom containing the bonding electron pairs in the molecule (Mason and Brady, 2007). It is expressed in degrees. The bond angle throws more light on the distribution of orbitals around a central atom in a molecule. The bond angles also contribute to the shape of a molecule.

It is observed that all the bond angles in Tetracene molecule are so closed to 120° in both gas phase and methanol suggesting that the molecule is planar benzene in which the C atom are sp^2 hybridized. In gas phase, the angles with least values include; A(12,18,26):C12-C18-H26, A(5,13,21):C5-C13-H21 and A(11,17,25):C11-C17-H25 with the values of 118.04° at RHF/3-21G and 118.357° at B3LYP/6-31G+ respectively. These are all C-C-H angles. But C-C-C angles: A(11,17,23):C11-C17-C23, A(11,5,13):C11-C5-C13 and A(5,11,17):C5-C11-C17 have values within 118.041° to 118.4556° at both levels of theory. In

methanol, the angles with the lowest values are A(12,18,26):C12-C18-H26, A(5,13,21):C5-C13-H21, A(11,17,25):C11-C17-H25 and A(6,14,22):C6-C14-H22 with the values ranging within 118.023° to 118.3218° at both levels of theory. These are all C-C-H angles. The C-C-C angles are; A (12, 6, 14), A (11, 5, 13) and A (5, 11, 17) with bond angles of 118.3891° , 118.4824° and 118.3885° respectively. This also shows that the values obtained in solution are a bit higher than the one obtained in gas phase by about 0.09° .

Table 3: Optimized Bond Angles (\AA) of Tetracene molecule in Gas.

Bond Angles	RHF				B3LYP			
	3-21G	3-21G+	6-31G	6-31G+	3-21G	3-21G+	6-31G	6-31G+
A(2,1,3)	118.9134	118.9134	118.8889	118.9009	118.8693	118.8897	118.8349	118.8444
A(2,1,4)	118.9127	118.9127	118.8884	118.9004	118.8693	118.8898	118.835	118.8445
A(2,1,4)	122.1739	122.1739	122.2227	122.1987	122.2614	122.2204	122.3301	122.3112
A(1,2,7)	118.9134	118.9134	118.8889	118.9009	118.8695	118.89	118.8351	118.8446
A(1,2,8)	118.9126	118.9126	118.8884	118.9004	118.8691	118.8896	118.8348	118.8443
A(7,2,8)	122.1739	122.1739	122.2227	122.1987	122.2614	122.2204	122.3301	122.3112
A(1,3,6)	121.6061	121.6061	121.7074	121.6912	121.8176	121.7958	121.9307	121.9169
A(1,3,9)	118.8061	118.8061	118.8063	118.8193	118.8519	118.8643	118.8139	118.8293
A(6,3,9)	119.5878	119.5878	119.4863	119.4895	119.3305	119.3399	119.2553	119.2538
A(1,4,5)	121.6066	121.6066	121.7077	121.6916	121.8177	121.7959	121.9308	121.917
A(1,4,10)	118.8045	118.8045	118.805	118.818	118.8518	118.8644	118.8138	118.8292
A(5,4,10)	119.589	119.589	119.4873	119.4905	119.3305	119.3396	119.2554	119.2539
A(4,5,11)	119.4808	119.4808	119.4039	119.4081	119.3131	119.3143	119.2343	119.2386
A(4,5,13)	122.1948	122.1948	122.2325	122.209	122.2637	122.2328	122.31	122.2964
A(11,5,13)	118.3243	118.3243	118.3636	118.3829	118.4232	118.4529	118.4558	118.465
A(3,6,12)	119.4805	119.4805	119.4037	119.4079	119.313	119.3143	119.2343	119.2386
A(3,6,14)	122.1945	122.1945	122.2322	122.2087	122.2637	122.2328	122.31	122.2963
A(12,6,14)	118.3251	118.3251	118.3641	118.3834	118.4233	118.4529	118.4558	118.465
A(2,7,12)	121.6062	121.6062	121.7075	121.6913	121.8176	121.7958	121.9307	121.9169
A(2,7,15)	118.8062	118.8062	118.8064	118.8193	118.8519	118.8643	118.814	118.8293
A(12,7,15)	119.5876	119.5876	119.4861	119.4894	119.3305	119.3398	119.2553	119.2538
A(2,8,11)	121.6064	121.6064	121.7077	121.6915	121.8177	121.7959	121.9308	121.9169
A(2,8,16)	118.8045	118.8045	118.8051	118.818	118.8514	118.8639	118.8135	118.8288
A(11,8,16)	119.5891	119.5891	119.4873	119.4905	119.3309	119.3402	119.2557	119.2542
A(5,11,8)	119.4808	119.4808	119.4039	119.4081	119.3131	119.3144	119.2344	119.2388
A(5,11,17)	118.3244	118.3244	118.3636	118.383	118.423	118.4527	118.4556	118.4648
A(8,11,17)	122.1948	122.1948	122.2324	122.209	122.2638	122.2329	122.31	122.2964
A(6,12,7)	119.4804	119.4804	119.4036	119.4078	119.313	119.3143	119.2343	119.2386
A(6,12,18)	118.3251	118.3251	118.3642	118.3835	118.4233	118.4529	118.4558	118.465
A(7,12,18)	122.1945	122.1945	122.2322	122.2087	122.2637	122.2328	122.31	122.2963
A(5,13,19)	121.039	121.039	121.0706	121.0684	121.0162	121.0259	121.0513	121.0644
A(5,13,21)	118.0398	118.0398	118.2163	118.2557	118.2282	118.2967	118.3131	118.357
A(19,13,21)	120.9212	120.9212	120.7131	120.6759	120.7556	120.6774	120.6356	120.5786
A(6,14,20)	121.0385	121.0385	121.0702	121.068	121.0161	121.0258	121.0512	121.0643
A(6,14,22)	118.041	118.041	118.2171	118.2566	118.2286	118.2971	118.3135	118.3574
A(20,14,22)	120.9206	120.9206	120.7126	120.6754	120.7553	120.677	120.6353	120.5783
A(11,17,23)	121.0388	121.0388	121.0705	121.0682	121.0162	121.0259	121.0513	121.0644
A(11,17,25)	118.0399	118.0399	118.2163	118.2557	118.2282	118.2967	118.3131	118.357
A(23,17,25)	120.9214	120.9214	120.7133	120.6761	120.7556	120.6774	120.6356	120.5786
A(12,18,24)	121.0384	121.0384	121.0702	121.068	121.0161	121.0258	121.0512	121.0643
A(12,18,26)	118.041	118.041	118.2171	118.2566	118.2286	118.2971	118.3134	118.3573
A(24,18,26)	120.9206	120.9206	120.7126	120.6755	120.7553	120.6771	120.6353	120.5783
A(13,19,23)	120.6367	120.6367	120.5658	120.5487	120.5606	120.5213	120.493	120.4706
A(13,19,27)	120.5385	120.5385	120.4621	120.4482	120.3243	120.329	120.2655	120.2521
A(23,19,27)	118.8248	118.8248	118.9722	119.0031	119.1151	119.1497	119.2415	119.2773
A(14,20,24)	120.6365	120.6365	120.5656	120.5485	120.5607	120.5213	120.493	120.4706
A(14,20,28)	120.5378	120.5378	120.4615	120.4477	120.3239	120.3286	120.2652	120.2517
A(24,20,28)	118.8257	118.8257	118.9729	119.0038	119.1155	119.1501	119.2418	119.2776
A(17,23,19)	120.6368	120.6368	120.5659	120.5488	120.5607	120.5214	120.4931	120.4707
A(17,23,29)	120.5385	120.5385	120.462	120.4482	120.3243	120.329	120.2655	120.2521
A(19,23,29)	118.8247	118.8247	118.9721	119.003	119.115	119.1496	119.2414	119.2773
A(18,24,20)	120.6365	120.6365	120.5656	120.5485	120.5607	120.5213	120.493	120.4706
A(18,24,30)	120.5378	120.5378	120.4615	120.4477	120.3239	120.3286	120.2652	120.2517
A(20,24,30)	118.8257	118.8257	118.9729	119.0038	119.1154	119.1501	119.2418	119.2776

Table 4: Optimized Bond Angles ($^{\circ}$) of Tetracene molecule (Methanol)

Bond Angles	RHF				B3LYP			
	3-21G	3-1G+	6-31G	6-1G+	3-21G	3-1G+	6-31G	6-31G+
A(2,1,3)	119.0126	119.0126	118.9767	118.9101	118.9604	118.9604	118.9134	118.9101
A(2,1,4)	119.0119	119.0119	118.9762	118.9101	118.9605	118.9605	118.9135	118.9101
A(2,1,4)	121.9756	121.9756	122.0471	122.1798	122.0791	122.0791	122.1731	122.1798
A(1,2,7)	119.0125	119.0125	118.9767	118.9102	118.9606	118.9606	118.9136	118.9102
A(1,2,8)	119.0118	119.0118	118.9762	118.9099	118.9603	118.9603	118.9133	118.9099
A(7,2,8)	121.9757	121.9757	122.0471	122.1798	122.0791	122.0791	122.1732	122.1798
A(1,3,6)	121.4083	121.4083	121.5329	121.768	121.6356	121.6356	121.7746	121.768
A(1,3,9)	118.8908	118.8908	118.8832	118.8958	118.9368	118.9368	118.8892	118.8958
A(6,3,9)	119.7009	119.7009	119.5839	119.3362	119.4277	119.4277	119.3362	119.3362
A(1,4,5)	121.4088	121.4088	121.5332	121.768	121.6357	121.6357	121.7746	121.768
A(1,4,10)	118.8891	118.8891	118.8818	118.8957	118.9366	118.9366	118.8891	118.8957
A(5,4,10)	119.7021	119.7021	119.585	119.3363	119.4277	119.4277	119.3363	119.3363
A(4,5,11)	119.5794	119.5794	119.4906	119.3219	119.4039	119.4039	119.3119	119.3219
A(4,5,13)	122.0321	122.0321	122.0908	122.1675	122.1137	122.1137	122.1831	122.1675
A(11,5,13)	118.3884	118.3884	118.4186	118.5107	118.4824	118.4824	118.505	118.5107
A(3,6,12)	119.5791	119.5791	119.4904	119.3219	119.4039	119.4039	119.3119	119.3219
A(3,6,14)	122.0317	122.0317	122.0905	122.1674	122.1137	122.1137	122.183	122.1674
A(12,6,14)	118.3891	118.3891	118.4191	118.5107	118.4824	118.4824	118.5051	118.5107
A(2,7,12)	121.4084	121.4084	121.533	121.768	121.6356	121.6356	121.7746	121.768
A(2,7,15)	118.8908	118.8908	118.8832	118.8958	118.9367	118.9367	118.8892	118.8958
A(12,7,15)	119.7007	119.7007	119.5838	119.3362	119.4277	119.4277	119.3363	119.3362
A(2,8,11)	121.4087	121.4087	121.5332	121.768	121.6356	121.6356	121.7746	121.768
A(2,8,16)	118.8891	118.8891	118.8819	118.8954	118.9362	118.9362	118.8887	118.8954
A(11,8,16)	119.7022	119.7022	119.5849	119.3366	119.4281	119.4281	119.3366	119.3366
A(5,11,8)	119.5794	119.5794	119.4906	119.322	119.404	119.404	119.3121	119.322
A(5,11,17)	118.3885	118.3885	118.4186	118.5105	118.4822	118.4822	118.5049	118.5105
A(8,11,17)	122.0321	122.0321	122.0908	122.1675	122.1137	122.1137	122.1831	122.1675
A(6,12,7)	119.579	119.579	119.4903	119.3219	119.4039	119.4039	119.3119	119.3219
A(6,12,18)	118.3892	118.3892	118.4192	118.5107	118.4825	118.4825	118.5051	118.5107
A(7,12,18)	122.0318	122.0318	122.0905	122.1674	122.1137	122.1137	122.183	122.1674
A(5,13,19)	120.9121	120.9121	120.9672	120.9383	120.8975	120.8975	120.9576	120.9383
A(5,13,21)	118.023	118.023	118.2043	118.3334	118.235	118.235	118.3214	118.3334
A(19,13,21)	121.0649	121.0649	120.8285	120.7283	120.8675	120.8675	120.7211	120.7283
A(6,14,20)	120.9117	120.9117	120.9668	120.9382	120.8974	120.8974	120.9574	120.9382
A(6,14,22)	118.0242	118.0242	118.2052	118.3338	118.2355	118.2355	118.3218	118.3338
A(20,14,22)	121.0642	121.0642	120.828	120.728	120.8671	120.8671	120.7208	120.728
A(11,17,23)	120.9119	120.9119	120.967	120.9383	120.8974	120.8974	120.9576	120.9383
A(11,17,25)	118.0231	118.0231	118.2044	118.3335	118.235	118.235	118.3214	118.3335
A(23,17,25)	121.065	121.065	120.8286	120.7283	120.8675	120.8675	120.721	120.7283
A(12,18,24)	120.9116	120.9116	120.9668	120.9381	120.8974	120.8974	120.9574	120.9381
A(12,18,26)	118.0242	118.0242	118.2053	118.3339	118.2354	118.2354	118.3218	118.3339
A(24,18,26)	121.0642	121.0642	120.828	120.728	120.8672	120.8672	120.7208	120.728
A(13,19,23)	120.6995	120.6995	120.6142	120.5511	120.6202	120.6202	120.5375	120.5511
A(13,19,27)	120.5259	120.5259	120.463	120.1846	120.3029	120.3029	120.2586	120.1846
A(23,19,27)	118.7747	118.7747	118.9228	119.2643	119.0769	119.0769	119.2039	119.2643
A(14,20,24)	120.6992	120.6992	120.6141	120.5511	120.6202	120.6202	120.5375	120.5511
A(14,20,28)	120.5251	120.5251	120.4623	120.1842	120.3025	120.3025	120.2583	120.1842
A(24,20,28)	118.7757	118.7757	118.9236	119.2646	119.0773	119.0773	119.2043	119.2646
A(17,23,19)	120.6996	120.6996	120.6143	120.5511	120.6203	120.6203	120.5375	120.5511
A(17,23,29)	120.5258	120.5258	120.4629	120.1846	120.3029	120.3029	120.2586	120.1846
A(19,23,29)	118.7746	118.7746	118.9228	119.2643	119.0768	119.0768	119.2039	119.2643
A(18,24,20)	120.6992	120.6992	120.6141	120.5511	120.6201	120.6201	120.5375	120.5511
A(18,24,30)	120.5251	120.5251	120.4623	120.1842	120.3025	120.3025	120.2583	120.1842
A(20,24,30)	118.7757	118.7757	118.9236	119.2646	119.0773	119.0773	119.2042	119.2646

HOMO-LUMO Energy Gap

Tables 5 and 6, show the calculated values of the HOMO, LUMO and HOMO-LUMO Energy gap in atomic unit (a.u) and in electron volt (eV) of the studied molecule in gas phase and in solution. It is clear from Table 5 and 6 that the HOMO-LUMO energy gap for the Tetracene molecule is approximately the same for all the basis sets at RHF level of the theory. At this theory, the energy gap is about 6.77864eV for the entire basis sets used. But it is observed that at B3LYP level of theory the energy gap for all basis sets

used is about 2.456eV for both gas and methanol. This value is more in agreement to a reported experimental value of 2.63 (Musa *et al.*, 2015). Thus, B3LYP calculations are more in agreement with the experimental value due to the inclusion of electron correlation than RHF. However, the average value of HOMO-LUMO energy gap in gas phase is 2.456eV which is slightly higher than the average value obtained in solution 2.455eV. This indicates that tetracene is slightly more stable in the gas phase than in solution form.

Table 5: HOMO-LUMO Energy of Tetracene Molecule in Gas Phase

Method	HOMO(a.u)	LUMO(a.u)	HOMO-LUMO Energy Gap (a.u)	HOMO-LUMO Energy Gap(eV)	HOMO-LUMO Energy Gap (eV) (Musa <i>et al.</i> , 2015).	
RHF	3-21G	-0.22449	0.02498	0.24947	6.78857764	
	3-21G+	-0.22449	0.02498	0.24947	6.78857764	
	6-31G	-0.22005	0.02788	0.24793	6.74667116	
	6-31G+	-0.21834	0.02917	0.24751	6.73524212	
B3LYP	3-21G	-0.17503	-0.08400	0.09103	2.4771836	
	3-21G+	-0.17503	-0.08400	0.09103	2.4771836	2.63
	6-31G	-0.17198	-0.08159	0.09039	2.4596268	
	6-31G+	-0.17096	-0.08239	0.08857	2.41016684	

Table:6 HOMO-LUMO Energy of Tetracene Molecule in solution (Methanol)

Method	HOMO (a.u)	LUMO (a.u)	HOMO-LUMO Energy Gap (a.u)	HOMO-LUMO Energy Gap(eV)	HOMO-LUMO Energy Gap (eV) (Musa <i>et al.</i> , 2015).	
RHF	3-21G	-0.22781	0.02125	0.24906	6.77742072	
	3-21G+	-0.22781	0.02125	0.24906	6.77742072	
	6-31G	-0.22172	0.02610	0.24782	6.74367784	
	6-31G+	-0.22004	0.02742	0.24746	6.73388152	
DFT	3-21G	-0.17800	-0.08701	0.09099	2.47601988	2.63
	3-21G+	-0.17800	-0.08701	0.09099	2.47601988	
	6-31G	-0.17288	-0.08251	0.09037	2.45914844	
	6-31G+	-0.17175	-0.08319	0.08856	2.40989472	

Mulliken Atomic Charges

The calculation of effective atomic charges plays an important role in the application of quantum mechanical calculations to molecular system because atomic charges affect dipole moment, molecular polarization, electronic structure, and a lot of properties of molecular system (Ciolowski *et al.*, 1998). The charge distribution over the atoms suggests the formation of donor and acceptor pairs involving the charge transfer in the molecule. Atomic charge has been used to describe the processes of electro negativity equalization and charge transfer in chemical reaction (Maksic and Jug, 1991). The interest here is in the comparison of different methods to describe the electron distribution in tetracene molecule as broadly as possible, and assess the sensitivity of the calculated charges to changes in (i) the choice of the basis set; (ii) the choice of the quantum mechanical method. Mulliken charges were calculated by determining the electron population of each atom as defined in the basic functions. The mulliken charges calculated for both gas phase and methanol are listed in Table 7. The data presented clearly shows that mulliken charges are very sensitive to basis set used in calculation. It is worthy to

mention that in the basis set 3-21G, all the hydrogen atoms of the title molecule exhibited positive charge values at RHF level of the theory in the gas phase while all carbon atoms exhibited negative charge values. H25 atom exhibits the highest positive charge value of 0.240669 in the gas phase while in methanol H15 atom exhibits the highest positive value of 0.283561 at RHF/3-21G. On the other hand, the maximum negative charge value of -0.267558 for C19 at RHF/3-21G. In methanol, it is observed that all the hydrogen atoms are positive charge values at RHF/3-21G level of theory. But at B3LYP/6-31G+, all the hydrogen atoms also have positive charge values while all the carbon atoms exhibited negative charge values with the exception of C5-C6 which possessed positive charge values of about 0.150176 and 0.149767 respectively. However, the presence of large negative charge value on C atom and large positive charge value on H atom may suggest the formation of intra molecular interaction in both forms (Rubarani and Sampath, 2013). Hence, it is also observed that the mulliken charges values in methanol are a bit higher in solution than in gas phase.

Table 7: Mulliken Atomic charge Distributions in Methanol and in Gas

Methanol			in Gas		
	RHF 3-21G	B3LYP 6-31G _s		RHF 3-21G	B3LYP 6-31G _s
Atoms	Charge (statC)	Charge (statC)	Atoms	Charge (statC)	Charge (statC)
C1	-0.120810	0.163157	C1	-0.097663	-0.097181
C2	-0.121025	0.163629	C2	-0.097893	-0.098746
C3	-0.171091	-0.326680	C3	-0.146332	-0.047966
C4	-0.170889	-0.326603	C4	-0.146135	-0.047932
C5	-0.120281	0.150176	C5	-0.097993	0.019146
C6	-0.120133	0.149767	C6	-0.097829	0.019567
C7	-0.170918	-0.326610	C7	-0.146167	-0.047671
C8	-0.170922	-0.326652	C8	-0.146164	-0.048182
H9	0.283547	0.165004	H9	0.240060	0.183377
H10	0.283555	0.165010	H10	0.240064	0.183389
C11	-0.120067	0.149755	C11	-0.097765	0.020386
C12	-0.120138	0.149721	C12	-0.097831	0.019587
C13	-0.217793	-0.229758	C13	-0.189051	-0.226265
C14	-0.217949	-0.229811	C14	-0.189209	-0.226150
H15	0.283561	0.165011	H15	0.240063	0.183385
H16	0.283558	0.165011	H16	0.240066	0.183386
C17	-0.217943	-0.229840	C17	-0.189195	-0.226984
C18	-0.217949	-0.229801	C18	-0.189211	-0.226340
C19	-0.267558	-0.161363	C19	-0.240755	-0.236637
C20	-0.267527	-0.161319	C20	-0.240731	-0.236236
H21	0.277569	0.161674	H21	0.240668	0.181051
H22	0.277567	0.161673	H22	0.240668	0.181045
C23	-0.267550	-0.161323	C23	-0.240753	-0.236079
C24	-0.267531	-0.161326	C24	-0.240732	-0.236280
H25	0.277561	0.161669	H25	0.240669	0.181044
H26	0.277567	0.161672	H26	0.240666	0.181044
H27	0.275886	0.159531	H27	0.242115	0.175555
H28	0.275904	0.159545	H28	0.242124	0.175563
H29	0.275898	0.159538	H29	0.242124	0.175561
H30	0.275901	0.159544	H30	0.242122	0.175563

Vibrational Frequencies and IR Intensities in Gas Phase and in Methanol

Spectroscopy is the study of matter and its interaction with electromagnetic radiation. All matter contains molecules; these molecules have bonds that are continually vibrating and moving around. These bonds can vibrate with stretched motions or bent motions (Mukamel, 2000). Infrared spectroscopy is the study of how molecules absorb infrared radiation and ultimately convert it to heat. Thus, IR spectra is the study of interaction of infrared light with matter. When a molecule absorbs infrared radiation, its chemical bonds vibrate and may either be stretched, contracted or bent (Villar *et al.*, 2012). The main focus of vibrational analysis is to get vibrational modes connected with the precise molecular structures of the measured compound (Hamm *et. al.*, 1998). Tables 8 and 9 show the calculated vibrational frequencies and intensities of the Tetracene molecule in the gas phase and in methanol.

From the values of the vibrational frequencies obtained in methanol, the first frequencies for DFT were negative which shows that the molecule was at first order saddle point or transition state on the potential energy surface. Whereas at RHF, where no

imaginary frequencies exist, the molecule was very stable. However, in the gas phase, no imaginary frequencies were found at both levels of theory indicating that the molecule would be more stable than in methanol.

In gas phase, the most intense frequency was found to be about 925cm^{-1} which occurred at an intensity of 146.7973 km/mol . At this frequency there is strong P-OR esters and medium RCOOH O-H bend mode of vibrations observed. The second most intense peak has frequency of about 1115cm^{-1} which occurred at the intensity of 113.4457 km/mol . At this frequency, strong C-F stretch, strong C-O stretch, medium C-N stretch and weak P=O phosphate mode of vibrations were observed. The third most intense frequency of about 3228cm^{-1} was observed at an intensity of 72.3565 km/mol . At this frequency, strong (broad) dimer OH, and strong broad ArO-H H-bonded mode of vibrations were observed. The fourth most intense peak has frequency of about 3226cm^{-1} which occurred at the intensity of 47.321 km/mol . At this frequency, strong (broad) dimer OH and strong broad ArO-H H-bonded mode of vibrations were observed. IRPal 2.0 was used to interpret these frequencies.

In Methanol, the most intense frequency was found to be about 390.1077 cm^{-1} which occurred at the intensity of 474.126 km/mol. At this frequency, strong C-Br and weak S-S disulfide asymmetric mode of vibrations were observed. The second most intense frequency of about 863 cm^{-1} was observed at an intensity of 201.4069 km/mol. At this frequency, there are medium C-H out of plane, strong S-OR esters and strong (broad) N-H wag amines mode of vibrations observed. Another most intense peak has frequency

of about 865 cm^{-1} which occurred at the intensity of 198.1175 km/mol. At this frequency, medium C-H out of plane and strong (broad) N-H wag amines mode of vibrations were observed. Another most intense peak has frequency of about 1088.5374 cm^{-1} at the intensity of 187.2281 km/mol. At this frequency, there are strong stretch, strong C-O stretch, medium C-N stretch and weak P-H bending mode of vibrations. IRPal 2.0 software was used to interpret these frequencies.

Table 8: Vibrational Frequencies and Intensities of Tetracene Molecule in Gas Phase

Mode	RHF				B3LYP			
	3-21G		6-31G		3-21G		6-31G	
	Frequency (cm^{-1})	Intensity (km/mol)						
1	75.6695	0.0000	56.2805	0.0000	60.8430	0.0000	76.4232	0.0000
2	92.6427	0.7087	85.8971	0.5090	55.9206	0.7459	47.4678	0.4992
3	187.9230	3.0238	184.4829	3.1824	158.0150	0.0000	153.0607	0.0000
4	207.1355	0.0000	199.5840	0.0000	161.1667	1.5555	157.5221	1.5577
5	207.9812	0.0000	203.1569	0.0000	162.4580	0.0000	160.0276	0.0000
6	341.2376	0.0000	343.1608	0.0000	299.6296	1.3706	300.6415	0.8515
7	350.8384	0.0000	346.7571	0.0000	305.4639	0.0006	304.5650	0.0009
8	358.3268	0.0027	352.9137	0.0006	315.2871	0.0000	311.0685	0.0000
9	360.7222	1.2829	357.7453	0.9339	326.9431	0.0000	327.9912	0.0000
10	464.4543	0.0000	461.3269	0.0000	401.7233	0.0000	399.5172	0.0000
11	518.7775	0.0044	513.7608	0.0011	470.8781	0.1375	465.8261	0.1327
12	561.9690	0.0002	556.8645	0.0000	485.6955	11.7628	489.5307	10.7455
13	562.5964	7.3444	560.4716	7.5839	488.1081	14.4726	495.7325	0.0000
14	572.7510	0.2114	571.9502	0.0043	490.2315	0.0091	497.1328	8.0731
15	573.1497	25.6793	573.9909	18.4977	522.8642	0.0001	517.9468	0.0000
16	607.7163	0.0002	605.2988	0.0002	523.9449	0.0000	527.2253	0.0001
17	611.2569	6.2553	614.6846	7.1597	586.6963	7.9413	585.4165	8.2483
18	666.1458	0.0000	659.3767	0.0000	592.5708	0.0000	585.7186	0.0021
19	688.6483	10.6211	685.2601	10.4330	647.2127	2.1495	641.6978	2.0416
20	718.3705	0.0000	713.5350	0.0000	672.3330	0.0000	666.9348	0.0000
21	726.3693	0.8831	720.8255	0.9683	678.7602	1.0234	673.0396	0.9722
22	819.5215	0.3140	830.7329	0.0000	730.8192	0.0000	733.4112	0.0000
23	833.9201	0.0000	849.3542	1.9150	768.7862	0.0003	771.6327	0.0002
24	851.0213	0.0002	862.0756	0.0000	776.9470	0.0001	774.1840	0.0000
25	870.2120	0.0000	872.8729	0.0000	780.6062	105.9127	783.8994	92.8634
26	885.0783	0.0000	879.4206	0.0000	787.4798	0.0002	785.1093	0.0088
27	901.4810	0.0000	896.3359	0.0000	813.4689	2.0032	819.2909	0.0001
28	909.5190	5.1830	912.4693	0.0013	819.0863	0.0001	822.9273	1.9479
29	914.6558	0.0013	922.7361	143.7864	822.1176	0.0001	826.1029	0.0003
30	924.9862	146.7973	973.8468	0.0000	871.0476	0.0000	877.1978	0.0000
31	956.5412	0.0000	1000.7977	1.2014	880.8517	0.0000	887.2268	0.0000
32	1006.8840	0.0001	1008.4999	0.0022	885.0250	0.0000	888.7298	0.0000
33	1024.3309	0.0000	1023.2253	0.0000	915.4883	0.0000	926.2123	0.0000
34	1033.7174	0.0000	1032.7025	0.0000	917.6460	0.0000	929.7441	0.0000
35	1050.7178	0.0000	1048.9363	0.0000	941.5385	89.3633	937.2543	0.0000
36	1053.6352	9.6136	1050.9970	9.4360	943.0296	0.0005	946.3282	77.1539
37	1081.3464	0.0000	1084.0315	0.0000	945.2638	0.0012	960.2049	0.0001
38	1114.4980	113.4457	1113.8769	115.1405	985.1732	2.3774	976.0189	2.3482
39	1121.7868	0.0002	1128.7643	0.0001	996.6672	0.0000	991.2499	0.7938
40	1122.8851	4.4718	1144.6443	5.2867	998.8674	14.9108	995.1016	22.2836
41	1125.0030	0.0005	1146.4864	0.0006	1031.5744	0.0001	1027.2202	0.0001
42	1171.2719	0.0001	1167.0585	0.0000	1031.7471	0.0001	1027.8227	0.0001
43	1174.3920	24.5417	1171.0136	31.6815	1076.5581	5.4585	1090.1132	6.3039
44	1201.0421	6.2710	1203.7112	0.0001	1076.8946	0.0054	1090.3157	0.0179
45	1203.6088	0.0002	1204.2953	0.0001	1149.7175	5.0099	1159.8028	5.3672

Table 8 continue

Mode	RHF				B3LYP			
	3-21G		6-31G		3-21G		6-31G	
	Frequency (cm^{-1})	Intensity (km/mol)						
47	1228.0843	0.0000	1241.2977	0.0000	1174.2296	0.0509	1206.1377	0.1951
48	1291.5950	0.0001	1316.1287	0.0000	1240.1708	0.0000	1231.8164	0.0000
49	1333.1109	0.5643	1335.1641	0.4239	1245.0785	0.9611	1240.1336	1.1601
50	1344.8399	0.0120	1355.7454	0.0001	1256.9308	0.0001	1257.3737	0.0001
51	1345.6901	0.0175	1363.9028	0.1933	1271.7312	0.0001	1279.2583	0.0817
52	1346.0218	0.5299	1365.9530	0.0001	1280.9731	0.0001	1290.7578	0.0001
53	1393.7309	0.0140	1423.8088	0.0064	1334.2248	0.0026	1340.6704	0.0018
54	1408.5003	0.0028	1424.3495	0.0103	1336.9371	0.0370	1346.3264	0.0225
55	1425.1873	7.9944	1439.6417	5.1020	1345.7677	1.9744	1357.7771	0.1288
56	1446.5942	9.6160	1449.8056	14.1745	1353.5709	18.5786	1358.4688	20.7360
57	1448.5680	14.8035	1451.4662	15.0375	1371.7520	15.1400	1378.3768	0.0032
58	1464.8907	0.0008	1480.9103	0.0003	1373.6588	0.1573	1399.5513	11.8050
59	1471.5965	0.0003	1510.7427	0.0002	1421.8969	0.0001	1477.0983	5.9877
60	1494.1931	1.8857	1568.4638	2.3926	1466.3713	2.5794	1478.3358	0.0005
61	1507.6691	0.0007	1578.2416	0.0007	1473.2364	0.0008	1511.7511	0.0001
62	1588.4187	3.6684	1592.4816	4.4876	1476.2162	5.5372	1519.6777	0.0013
63	1616.2771	0.0000	1627.1036	0.0001	1511.9136	0.0001	1525.1774	2.2136
64	1647.7492	0.0000	1654.4165	0.0000	1539.9075	0.0000	1563.4515	0.0003
65	1662.0585	18.7208	1683.7949	1.9024	1562.2533	3.9007	1580.3779	3.2581
66	1665.7993	1.8934	1687.2065	14.7786	1566.0620	10.5868	1591.1559	6.8071
67	1694.3167	0.0018	1730.9724	0.0009	1601.0169	0.0008	1631.9770	0.0004
68	1718.0578	0.0018	1760.6674	0.0014	1622.6562	0.0019	1659.5786	0.0009
69	1723.8560	6.4557	1768.1054	6.5970	1626.2588	2.0521	1664.4215	1.6165
70	1726.6887	0.0015	1776.4761	0.0010	1633.3695	0.0010	1676.7261	0.0009
71	1750.7824	0.0083	1805.1828	0.0361	1634.2921	0.0007	1680.4959	0.0004
72	1756.9810	25.7739	1808.0353	22.2400	1653.3774	7.8908	1696.3615	6.3086
73	3183.3616	0.0000	3202.7526	0.0000	3137.6595	0.0000	3156.6657	0.0000
74	3185.4751	1.3874	3204.8192	1.7820	3139.7705	1.2290	3158.7936	1.6990
75	3189.1264	9.2173	3208.2650	17.8349	3141.6380	16.2330	3160.3750	31.1390
76	3191.8321	0.0001	3211.0957	0.0001	3144.1933	0.0000	3163.2153	0.0001
77	3202.6558	5.7130	3219.9535	10.9950	3156.4084	0.0061	3173.6550	0.0272
78	3202.8069	0.0007	3220.1097	0.0039	3156.4509	14.2584	3173.7075	24.5772
79	3205.7724	5.4234	3223.7841	4.8693	3158.7980	5.4436	3176.6969	5.4351
80	3206.4747	0.0001	3224.6236	0.0002	3159.2023	0.0000	3177.2038	0.0001
81	3227.5948	3.0247	3244.8604	0.0050	3181.2489	0.1871	3198.5211	0.0131
82	3227.6215	47.2311	3244.9226	73.0343	3181.2534	35.6343	3198.5499	62.1495
83	3248.3453	72.3565	3266.9563	116.1227	3199.7416	63.1105	3218.5891	108.2845
84	3248.6157	0.0018	3267.3411	0.0014	3199.9455	0.0006	3218.9013	0.0003

Table 9: Vibrational Frequencies and Intensities of Tetracene Molecule in Methanol.

Mode	RHF				B3LYP			
	3-21G		6-31G		3-21G		6-31G	
	Frequency (cm^{-1})	Intensity (km/mol)						
1	65.9403	1.6433	63.5472	1.2546	-61.7171	1.5152	-60.0284	1.0042
2	104.3894	0.0002	101.5053	0.0002	96.1945	0.0001	93.8897	0.0001
3	170.0060	0.0001	169.0852	0.0001	155.1964	0.0002	156.4318	0.0002
4	175.6798	2.8932	176.5595	3.4279	164.7723	0.0800	165.4692	2.3408
5	214.8220	0.0001	213.1757	0.0000	198.6345	0.0001	198.9881	0.0000
6	298.4672	1.6716	299.5439	1.1931	275.9632	1.7751	280.2008	1.0598
7	335.2587	0.0000	334.2823	0.0000	311.0720	0.0000	310.7234	0.0000
8	340.4258	0.0000	339.9878	0.0000	320.6282	0.0000	320.0591	0.0000
9	356.7476	0.0001	354.8946	0.0000	326.8650	0.0000	328.0300	0.0000
10	426.0629	0.0000	425.4724	0.0001	0.1170	458.8012	390.7004	0.0000
11	496.2697	0.0101	492.4624	0.0012	390.1077	474.1260	456.3864	0.1328
12	526.8400	85.9214	529.5507	72.5912	474.1260	53.8238	484.3646	42.3109
13	534.4352	0.0001	536.3439	0.0001	481.0749	0.0000	489.3288	0.0000
14	550.5677	0.1011	550.8965	0.0019	487.9860	4.1601	495.3102	0.9519
15	557.0304	0.0000	554.1061	0.0000	518.0187	0.0000	515.2024	0.0000
16	577.2554	0.0004	578.2629	0.0003	525.8151	0.0003	531.6542	0.0002

Table 9 continue

Mode	RHF				B3LYP			
	3-21G		6-31G		3-21G		6-31G	
	Frequency (cm^{-1})	Intensity (km/mol)						
17	611.3406	10.4052	608.2750	10.9314	573.1936	15.1059	570.4339	15.5773
18	634.9135	0.0000	630.1016	0.0000	584.6554	0.0000	580.5804	0.0000
19	668.9787	11.9346	669.1502	11.9324	630.4100	3.6157	628.5219	3.4056
20	692.3884	0.0000	689.8150	0.0000	647.0709	0.0000	644.4719	0.0000
21	707.1946	2.0796	703.3919	2.0659	657.9946	1.9656	654.8323	2.0477
22	762.7755	1.4279	787.8042	3.1533	742.9551	0.0000	746.8473	0.0000
23	812.8106	0.0000	823.8376	0.0000	745.6495	2.5506	759.2788	3.1413
24	835.7624	0.0001	832.1762	0.0001	754.6934	0.0000	764.7443	0.0000
25	852.2046	0.0000	850.1988	0.0000	758.7332	0.0000	765.5827	0.0000
26	853.2378	0.0000	857.3735	0.0000	771.0841	151.6191	778.2413	139.3628
27	864.8877	198.1175	862.6598	201.4069	783.5573	0.0004	781.9944	0.0002
28	875.9888	0.0000	869.4559	0.0001	792.5597	0.0000	790.9094	0.0000
29	890.1298	0.0000	882.5929	0.0000	799.2529	0.0000	799.5257	0.0000
30	912.9082	0.0000	928.5097	0.0000	858.1184	0.0000	870.7280	0.0000
31	975.7099	0.0000	972.7980	0.0000	867.2656	0.0000	874.0809	0.0000
32	983.0928	0.0001	980.6177	0.0000	874.6317	0.0000	882.3976	0.0000
33	1001.8938	0.0000	1001.4704	0.0000	888.3667	0.0000	892.2106	0.0000
34	1029.7773	0.0000	1024.7324	0.0000	915.1815	0.0003	922.9333	0.0000
35	1031.0676	7.6401	1040.3844	14.2760	927.6901	0.0000	924.8769	0.0001
36	1044.0444	13.9690	1055.4251	0.0000	941.3440	143.9040	946.6025	138.2008
37	1048.6446	0.0000	1067.2016	5.3807	943.7424	0.0000	955.7919	0.0000
38	1056.9567	0.0001	1079.8287	0.0000	967.3464	5.0057	959.7271	5.0690
39	1092.8134	170.1864	1088.5374	187.2281	1003.4686	0.0000	998.7773	0.0000
40	1102.8570	0.0000	1102.9875	0.0000	1004.4480	14.5676	1000.6011	22.2337
41	1119.4012	0.7145	1148.9339	0.0001	1011.5808	5.1424	1029.8416	0.0005
42	1156.7998	0.0001	1150.8871	29.8210	1012.4524	0.0003	1030.2022	0.0232
43	1158.3420	22.1757	1157.4505	0.4788	1032.3471	0.0000	1030.9573	5.6923
44	1182.9375	0.0000	1179.9321	0.0000	1032.4531	0.0000	1031.4885	0.0002
45	1183.1881	0.0002	1180.3246	0.0001	1152.2236	5.5843	1161.4175	5.9264
46	1217.6095	9.9409	1238.8780	11.5871	1161.0725	0.0000	1164.6434	0.0000
47	1241.3647	0.0000	1251.0120	0.0000	1167.7971	1.2581	1190.1632	4.1511
48	1286.8325	0.0000	1296.2914	0.0000	1207.4722	0.0000	1207.0867	0.0000
49	1298.3017	2.7466	1299.0911	1.3460	1211.0938	1.7328	1208.8055	2.9187
50	1325.1267	0.0000	1327.9538	0.0000	1238.6841	0.0000	1237.3958	0.0000
51	1329.5214	1.1285	1332.1292	0.8050	1241.5228	0.0000	1247.8049	0.2350
52	1329.9905	0.0002	1334.2722	0.0000	1243.3848	0.2724	1252.2318	0.0000
53	1382.5388	12.7565	1410.0319	18.2905	1321.6256	41.4754	1322.1373	0.0000
54	1413.5084	29.2231	1423.7840	0.0001	1321.9787	2.6366	1327.7179	27.8111
55	1426.1490	0.0000	1425.4423	25.8298	1323.7697	0.0000	1335.3770	17.3012
56	1441.1866	22.3628	1443.2697	5.6010	1338.1971	3.7734	1340.8154	1.5840
57	1449.4963	2.4017	1448.9771	16.2923	1364.4044	38.2259	1381.6352	0.0000
58	1462.9684	0.0001	1493.2152	0.0000	1378.4352	0.0000	1391.5480	30.2454
59	1486.3476	0.0000	1519.2777	0.0000	1383.2384	0.0000	1431.1775	0.0000
60	1545.3725	0.0000	1554.1345	4.8458	1416.3897	3.4192	1445.4247	9.7113
61	1549.5463	7.7489	1576.1985	0.0000	1417.2527	0.0000	1449.6704	0.0000
62	1552.8718	4.5246	1585.3940	2.6095	1446.9039	9.8386	1451.5326	0.0005
63	1594.9916	0.0000	1612.6128	0.0000	1490.2801	0.0000	1500.2062	0.0000
64	1604.3431	0.0001	1613.2604	0.0000	1494.9627	0.0000	1502.2383	0.0000
65	1612.0338	17.0229	1627.8805	12.4841	1508.9277	21.4157	1521.6332	14.4307
66	1686.6079	0.0000	1708.3085	0.0000	1549.8496	0.0000	1573.4253	0.0000
67	1707.5241	0.0000	1738.0254	16.7709	1555.7108	0.0000	1586.9237	0.0000
68	1710.4738	9.6904	1740.9946	0.0001	1568.4970	4.5015	1596.5246	7.6228
69	1744.5357	0.8707	1764.6042	2.1923	1601.6478	3.7771	1620.9592	4.2633
70	1783.0433	0.0000	1814.8307	0.0000	1629.7112	0.0000	1664.2879	0.0000
71	1816.7212	0.0002	1845.2921	0.0001	1651.6386	0.0000	1674.7071	0.0000
72	1824.6086	36.3172	1852.0569	30.7307	1661.6186	23.2315	1689.4019	16.3068
73	3291.9954	0.0000	3302.6135	0.0000	3128.4323	0.0000	3140.2708	0.0000
74	3293.9965	1.1666	3304.6177	1.6286	3130.4255	0.7172	3142.3143	1.3007
75	3296.1813	0.7812	3306.0896	2.4302	3131.6972	0.1442	3143.0801	5.1239

Table 9 continue

Mode	RHF				B3LYP			
	3-21G		6-31G		3-21G		6-31G	
Frequency (cm^{-1})	Intensity (km/mol)							
76	3298.2231	0.0000	3308.3923	0.0000	3133.5125	0.0000	3145.1849	0.0000
77	3301.6944	8.7199	3308.7474	0.0000	3138.9097	0.0128	3146.6547	0.0001
78	3301.7518	0.0059	3309.0538	0.6935	3138.9194	1.1773	3146.7678	1.5903
79	3304.7759	10.4108	3312.7454	7.4096	3141.2192	8.0121	3149.9650	6.8743
80	3305.3161	0.0001	3313.5922	0.0000	3141.4629	0.0002	3150.3945	0.0001
81	3321.3662	3.7444	3329.1188	0.0314	3156.8706	8.5082	3165.0512	32.7862
82	3321.3677	9.5537	3329.1386	36.6543	3156.8916	0.0011	3165.0534	0.3408
83	3333.5513	12.0362	3341.8215	42.6573	3168.6687	5.5319	3177.7177	34.8536
84	3333.6158	0.0009	3341.9557	0.0011	3168.6990	0.0005	3177.8109	0.0009

CONCLUSION

The optimized parameters (bond lengths and bond angles) of the tetracene molecule were calculated. The results obtained showed that the lowest average value of bond length was 1.072Å at RHF/3-21G and at DFT was 1.085Å in the gas phase. In methanol, the lowest average value was obtained to be 1.075Å using RHF and at DFT level, it was 1.087Å. Optimized bond angle was found to be approximately 120° in both gas phase and methanol suggesting that the molecule is planar benzene in which the C atoms are sp^2 hybridized. The calculated HOMO-LUMO Energy gap showed that the molecule will be more stable in chemical reaction in the gas phase than in methanol. The DFT values of HOMO-LUMO gap appeared to be closer to the reported experimental value of 2.63eV than those obtained by RHF method. The Mulliken atomic charges were found to be very sensitive to the basis sets used at both levels of theory. The results also indicated that at RHF/3-21G, all the hydrogen atoms exhibited positive charge values while all the carbon atoms exhibited negative charge values. The vibrational frequencies and intensities were calculated and the results obtained show that tetracene molecule would be more stable in the gas phase than in methanol as a result of the fact that no imaginary frequencies were observed in the gas phase. It is also found that, the most intense frequency was 924.9862 cm^{-1} which occurred at the intensity of 146.797 km/mol with RHF/3-21G in gas

REFERENCES

- Anna K. and Heinz B. (2015), "Electronic Processes in Organic Semiconductors" First Edition. Wiley-VCH Verlag GmbH & Co. KGaA. Published by Wiley-VCH Verlag GmbH & Co. KGaA pp
- Cioslowski, J. (1998) "Encyclopedia of Computational Chemistry", ed. P. v. R. Schleyer, N. L. Allinger, T. Clark, J. Gasteiger, P. A. Kollman, H. F. Schaefer III, Wiley, New York, vol. 5, p. 892
- Denniston, K. J., Topping, J., and Dwyer, T. M, (2007) "General organic and Biochemistry", 5th Edition, Towson University.
- Frisch M. J., Trucks, G.W., Schlegel H. B., Scuseria G. E., Robb M. A., Cheeseman J. R., Montgomery J. A. Jr., Vreven, T., Kudin K. N., Burant, J. C., Millam, J. M., Iyengar S. S.

phase while at B3LYP/3-21G has the most intense frequency of 474.1260 cm^{-1} occurring at an intensity of 390.107 km/mol in methanol.

RECOMMENDATIONS

The authors recommend that other levels of theory and higher basis sets should be used to carry out the computations. Another molecular modelling tool can also be used to perform all the calculations and also to compute Raman frequencies and spectra of the molecule. Comparison should be made with this work.

CONTRIBUTIONS OF AUTHORS

A.S Gidado initiated the work, provided some relevant journals and performed the optimization calculations in both gas and methanol. Abubakar Maigari carried out the calculations for vibrational frequencies in both gas and methanol and also provided some relevant journals for review while G.S.M Galadanci did the calculations of HOMO-LUMO energy gaps and Mulliken atomic charges of the molecule in both gas and methanol. We all took part in the compilation and interpretation of the results as well as the proof reading of the entire write up.

Acknowledgement

The authors wish to thank Dr. Chifu E. Ndikilar of the department of Physics, Federal University Dutse, Jigawa state for providing them with the Guassian 03 package.

,Tomasi, J. , Barone, V. , Mennucci B., Cossi, M., Scalmani, G. , Rega, N. , Petersson, G. A., Nakatsuji , H., Hada, M., Ehara, M., Toyota, K., Fukuda, R., Hasegawa, J., Ishida, M., Nakajima, T., Honda, Y., Kitao, O., Nakai, H., Klene, M., Li, X., Knox, J. E., Hratchian, H. P., Cross, J. B., Bakken, V., Adamo, C., Jaramillo, J., Gomperts, R., Stratmann, R. E., Yazyev, O., Austin, A. J., Cammi, R., Pomelli, C., Ochterski, J. W., Ayala, P. Y., Morokuma, K., Voth, G. A., Salvador, P., Dannenberg, J. J., Zakrzewski, V. G., Dapprich, S., Daniels, A.D., Strain, M. C., Farkas, O., Malick, D. K., Rabuck, A. D., Raghavachari, K., Foresman, J. B., Ortiz, J. V., Cui, Q., Baboul, A. G., Clifford, S., Cioslowski, J., Stefanov, B. B., Liu, G., Liashenko, A., Piskorz, P., Komaromi,

- I., Martin, R. L., Fox, D. J., Keith, T., Al-Laham, M. A., Peng, C.Y., Nanayakkara, A., Challacombe, M., Gill, P.M.W., Johnson, B., Chen, W., Wong, M.W., Gonzalez, C., Pople, J. A. (2004). "Gaussian 03", Gaussian, Inc., Wallingford C. T.
- Gidado A.S, Bbabaji G. and Ado M. (2015), "Determination of Vibrational Frequencies, HOMO-LUMO Energy and IR-Spectra of Nucleobases (Adenine, Cytosine, Guanine, Thymine and Uracil)" J.NAMP vol **31** pp 465-476.
- Hamm, P. , Lim, M. and Hochstrasser, R. M (1998). "Structure of the amide 1 bond of peptides measured by Femtosecond nonlinear-infrared spectroscopy". J. Phys. Chem. B 102 (31): PP 6123.
- Hoover, R. (2014). "Need to Track Organic Nano-Particles Across the Universe? NASA's Got an App for That". NASA. Retrieved February 22, 2014.
- Maksic, K. and Jug, Z. B. (1991). "Theoretical Model of Chemical Bonding", Ed. Z.B. Maksic, Part 3, Springer, Berlin , p. 29, p. 233.
- Mukamel, S. (2000). "Multidimensional femtosecond correlation spectroscopies of Electronic and Vibrational Excitations". Annual Review of physical chemistry. 51(1) PP 691-729.
- Mason, P. E. and Brady, J. W. (2007). "Tetrahedrality and the Relationship between Collective Structure and Radial Distribution Functions in Liquid Water". J. Phys. Chem. Vol. 111 (20) pp 5669–5679.
- Mason, Z-T. Zuh, J.T. R. Dieckmann, G.G. Malliara(2002) Appl. Phys, Lett, 81, pp. 4643-4645.
- Musa, A. M. A., Saeed, A., Shaari, R. S. and Lawal, M. (2015). " Effects of delocalized π -electrons around the linear acenes ring ($n = 1$ to 7): an electronic properties through DFT and quantum chemical descriptors", Molecular Physics: An International Journal at the Interface between Chemistry and Physics, DOI:10.1080/00268976.2014.993734.
- Peter, I. D., Elizabeth I. M., Stephen, R. F. , Mark, E. T., (2009). "Measurement of the lowest unoccupied molecular orbital energies of molecular organic semiconductors" *Organic Electronics* 10 515–520.
- Rubarani, P., Gangadharan and S. Sampath Krishnan 20013 "Natural Bond Orbital (NBO) Population Analysis of 1-Azanaphthalene-8-01 ACTA Physical Vol. 125, PP 18-22.
- Shaw and Seidler (2001) "Organic electronics: Introduction" IBM Res. & Dev. Vol 45, PP 179-182
- Suzuki S.; Morita Y.; Fukui K.; Sato K.; Shiomi D.; T.; Nakasuji K. (2006) 'Aromaticity on the pancake-bonded Dimer of Neutral phenalenyl Radical as studied by MS and NMR Spectroscopies and NICS Analysis' J. Am. Chem. Soc. 128 (8): 2530-2531.
- Takahashi, T. T. Takenobu, J. Takeya, Y. I. (2007). "Ambipolar Light-Emitting Transistors of a Tetracene Single Crystal". Advanced Functional Materials **17** (10): 1623–1628. doi:10.1002/adfm.200700046.
- Villar, A.; Gorritxategi, E. , Aranzade, E. ; Fernandex, L. A (2012). "Low-cost visible-near infrared sensor for on-line monitoring of fat and fatty acids content during the manufacturing process of the milk". Food Chemistry. 135(4): PP 2756-2760. Doi : 10.16/ j. food chem.. 2012.074.